International Journal of Science and Research (IJSR)
ISSN: 2319-7064
Impact Factor 2025: 7.089

Green Synthesis of Ag & Cu Nanoparticles from Waterlily (*Nymphaea spp.*) Plant: Characterization and their Biotechnological Applications

Praveen Pathak, Dr Sandeep Kumar Verma

Abstract: ***This study investigates the effects of green synthesized copper nanoparticles (CuNPs) and silver nanoparticles (AgNPs) on the secondary metabolites of the herb Bacopa monnieri. Nanoparticles were synthesized using waterlily leaf and characterized via XRD, FTIR, DLS, UV-visible spectrophotometry and SEM, revealing spherical particles with diameters between 20 nm and 1 µm. Experimentation with Murashige and Skoog medium showed that thidiazuron (TDZ) at 1.0 mg L-1 was most effective, yielding 8 shoots per explant. The combination of TDZ with AgNPs at 20 mg L-1 significantly increased shoot production to 10 shoots per explant. Analysis of methanolic extracts indicated a concentration-dependent rise in secondary metabolites, with an optimal range of 20-40 mg L-1, before reaching toxic levels at 50 mg L-1. Reactive oxygen species (ROS) indicators and antioxidant enzyme activity increased, suggesting that sub-toxic concentrations of CuNPs and AgNPs enhance Bacopa monnieris secondary metabolism and antioxidant capacity.***

Keywords: Green synthesis; Silver nanoparticles; Copper nanoparticles; Waterlily; Bacopa monnieri; Secondary metabolites; Reactive oxygen species; Nanobiotechnology.

1. Introduction

Nanobiotechnology integrates plant biotechnology, nanoscience and green chemistry to enhance agricultural productivity and the biosynthesis of medicinal metabolites. Key nanomaterials, such as AgNPs and CuNPs, exhibit unique properties like antimicrobial action and catalytic activity but involve hazardous reagents in traditional synthesis. Green synthesis using plant extracts offers a safer, eco-friendly alternative [1]. Waterlily lotus (*Nymphaea spp.*), rich in polyphenols and flavonoids, serves as an effective reducing and stabilizing agent for nanoparticle formation, resulting in biocompatible and bioactive phytogenic nanoparticles.

Characterization techniques including UV-Vis spectrophotometry, X-ray diffraction (XRD), and scanning electron microscopy (SEM) confirm the nanoparticles formation and morphology, typically showing spherical shapes with varied sizes. *Bacopa monnieri* (Brahmi), a medicinal herb known for its cognitive-enhancing properties, contains diverse secondary metabolites like bacosides, which improve memory and support brain health. Bacosides enhance synaptic transmission and nerve conduction, showing potential for managing neurological conditions such as Alzheimer's and Parkinsons disease. The herb also exhibits anxiolytic and antidepressant effects by modulating neurotransmitters and reducing cortisol levels without sedative effects [2].

Bacopa monnieri, known for its neuroprotective properties, exhibits strong antioxidant activity by enhancing endogenous enzymes like superoxide dismutase (SOD), catalase (CAT), and glutathione peroxidase (GPX), while lowering malondialdehyde (MDA) levels, thereby protecting tissues from oxidative damage. Its antioxidant capacity contributes to various protective effects, including anti-aging, hepatoprotection, cardioprotection and nephroprotection. The plant also possesses anti-inflammatory, anti-ulcer, antidiabetic, antimicrobial and anticancer properties, largely attributed to its phenolic and flavonoid compounds. Extracts have shown efficacy against pathogens like Staphylococcus aureus and *E. coli* and have induced apoptosis in cancer cells such as those from breast, lung and colon cancers. In Ayurveda, *B. monnieri* is utilized to treat disorders like epilepsy, anxiety, asthma, digestive issues and cardiovascular weaknesses, with classical formulations still in use. The plants therapeutic effects stem from its secondary metabolites, particularly bacosides, flavonoids and phenolic acids, which provide neuroprotective, adaptogenic, immunomodulatory and antioxidant benefits [3].

Current research focuses on enhancing bacoside production through plant tissue culture and nanoparticle elicitation. Nanoparticles can boost reactive oxygen species (ROS) generation, facilitating the activation of defense-related pathways and phenylpropanoid metabolism. Cytokinins such as thidiazuron (TDZ) are crucial in promoting shoot organogenesis and combining TDZ with nanoparticles could improve morphogenesis and secondary metabolite yield. Moderate ROS levels at sub-lethal nanoparticle concentrations stimulate antioxidant and metabolic enzyme activity, enhancing phenolic and flavonoid synthesis. However, excessive ROS can lead to metabolic toxicity and impaired growth. Given Bacopas medicinal value and the rising demand for bacoside-rich material, sustainable strategies to enhance secondary metabolite production are essential.

This research provides new insights into the biotechnological use of phytogenic AgNPs and CuNPs as metabolic elicitors and growth enhancers in medicinal plants. The findings demonstrate the potential of nanoparticle-mediated modulation of ROS signaling to improve secondary metabolite biosynthesis in *B. monnieri*, offering a promising strategy for producing high-value phytochemicals under controlled in vitro conditions.

2. Materials and Method

Preparation of Plant Extract

Fresh waterlily leaves (25 grams) were collected from SAGE University Indore, washed with double distilled water and cut into small pieces. It was ground to a smooth solution with 50 mL of distilled water and then heated in a water bath at 80°C for 5 min. The mixture was filtered through Whatman filter paper No. 1 and centrifuged at 5000 rpm for 10 min to obtain the supernatant used for the nanoparticle production.

2.1.1 Synthesis of Silver and copper nanoparticles from waterlily *(Nymphaeaceae)* plant extract:

This procedure outlines the synthesis of metal nanoparticles (MNPs) using waterlily leaf extract. A mixture of 20 mL supernatant from the extract and 5 mL of 1 mM silver nitrate ($AgNO_3$) and copper sulphate ($CuSO_4$) was kept at room temperature in the dark for 24 hours, resulting in a color change from ($AgNO_3$) white to dark brown and ($CuSO_4$) lite blue to brown, indicative of a reaction. The mixture was then centrifuged at 12,000 rpm for 30 minutes and the pellet was collected, oven-dried, crushed into powder and stored for further characterization. These synthesized materials are then applied as growth inducer for *in vitro* grown *Bacopa monnieris* supplemented in Murashige and Skoog (1962) medium [4].

2.1.2 Surface sterilization and culture conditions

Seeds of *Bacopa monnieri* underwent surface disinfection with 20% bleach plus Tween-20 for 10 minutes using a sonicator, followed by rinsing with sterile distilled water. Approximately 20-40 seeds were cultured aseptically on Murashige and Skoog medium (1962) with 3% sucrose, solidified after pH adjustment to 5.8. Cultures were kept at 23 ± 1°C in darkness for 2 days, then moved to a 16h light:8h dark photoperiod at 60% humidity. Hypocotyl segments from 21-day-old seedlings were utilized as explants for culture initiation.

2.1.3 Preparation of Culture Media for Shoot Regeneration

Shoot regeneration medium was prepared using Murashige and Skoog (MS) medium with 3% sucrose and 0.01% myo-inositol and supplemented with 0-2 mg L-1 6-benzyladenine (BA), TDZ, Zeatin, or Kinetin. The pH was adjusted to 5.7, and 0.7% gelling agent was added and autoclaved at 1.1 kg cm-2 and 121 °C for 20 minutes. Experiments were repeated three times with 20 replicates each, totaling 60 explants per treatment. The frequency of explants developing shoots and the mean number of shoots per explant were recorded after five weeks of culture.

2.1.4 Exposer of CuNPs and AgNPs on Shoot Culture

Hypocotyl-derived shoots were placed on MS medium with 1.0 mg L-1 TDZ alongside varying concentrations of CuNPs and AgNPs (0-50 mg L-1) for five weeks. Matured shoots were then harvested and dried for biochemical analysis.

2.1.5 Extraction of Secondary Metabolites

Secondary metabolites were extracted using methanol by combining 30 ml of 70% methanol with 1 gram of dry powdered BM plant in a 100 ml flask and refluxing at 95°C for 30 minutes. The extraction process included adding 30 ml of 70% methanol twice, followed by filtering with Whatman filter paper No. 41, yielding a total volume of 100 ml. After evaporation using a rotary evaporator, the recovery rate of extraction was approximately 50–60%.

2.1.6 Estimation of Total Saponin Content (TSC)

The vanillin-sulphuric acid method, modified by Bhardwaj et al. (2016), quantifies total saponins content (TSC) spectrophotometrically. It involves mixing 0.125 ml of methanolic extract, 1.25 ml of 72% sulfuric acid and 0.125 ml of an 8% vanillin solution. The mixture is incubated at 60°C for 10 minutes then cooled in ice before measuring absorbance at 544 nm using a Mecasys Optizen POP UV-visible spectrophotometer. Saponin serves as the standard for the curve, with results expressed in mg of saponins per gram of dry plant weight and a detection range of 0–400 µg of saponin.

2.1.7 Estimation of Total Alkaloid Content (TAC)

The TAC was measured spectrophotometrically using Dragendorffs reagent. A 5 mL methanolic extract was adjusted to pH 2-3 with diluted HCl. After adding 2 mL of Dragendorffs reagent, the mixture was centrifuged and the supernatant was decanted. The precipitate was washed with ethanol and treated with 2 mL of 1% disodium sulfide, resulting in a brownish-black precipitate that was further centrifuged. Two drops of disodium sulfide were added to confirm complete precipitation. The mixture was warmed and dissolved in 2 mL of strong nitric acid, diluted to 10 mL and combined with 5 mL of a 3% thiourea solution. Absorbance was measured at 435 nm, with results expressed as mg of $Bi(NO_3)_3$. 5H2O equivalent per gram of dry plant weight, using bismuth nitrate pentahydrate for the standard curve [5].

2.1.8 Estimation of Total Phenolic Content (TPC)

The Folin-Ciocalteu reagent method, modified by Bhardwaj et al. (2016) from Ainsworth and Gillespie (2007) [6]-[7], estimates total phenolic content (TPC) spectrophotometrically. The procedure involves mixing 1.25 ml of 0.2N Folin-Ciocalteu reagent, 1 ml of 7.5% sodium carbonate, and 25 µl of methanolic extract, then measuring the absorbance at 765 nm after three-hour incubation in the dark. A calibration curve using gallic acid establishes the results, reported as mg gallic acid equivalent per gram of the plants dry weight.

2.1.9 Estimation of Total Flavonoid Content (TFC)

Using aluminum chloride, spectrophotometric analysis estimated total flavonoid content (TFC) by combining specific volumes of methanol, aluminum chloride, potassium acetate and distilled water with a methanolic extract. After resting for 30 minutes at room temperature, absorbance was measured at 415 nm against a blank. Quercetin facilitated the creation of a standard curve, with results expressed as µg quercetin equivalent per gram of plant dry weight [8].

2.2 Estimation of DPPH radical scavenging capacity (DRSC)

1,1–diphenyl 2–picrylhydrazyl (DPPH) was utilized to assess the radical scavenging capacity (DRSC) of a methanolic extract. The antioxidant capability of the plant extract was evaluated using the DRSC test, which involved incubating 50

µl of methanolic extract with 950 µl of a 100 µM DPPH solution for 30 minutes at 37°C. Absorbance was measured at 517 nm via spectrophotometry to calculate the percentage of radical scavenging activity, using a methanol-treated control for comparison.
DRSC % = Ac − As /Ac × 100,

Whereas represents the absorbance of the sample or standard and Ac denotes the absorbance of the control. Ascorbic acid was utilized as the standard, with findings expressed in milligrams of ascorbic acid equivalent per gram of the plants dry weight (mg gm−1) [6].

2.2.1 Determination of hydrogen peroxide and malondialdehyde (MDA) contents

The study utilized spectrophotometry to assess oxidative stress indicators, specifically hydrogen peroxide (H_2O_2) and malondialdehyde (MDA), in fresh shoot tissues from control and BM plants treated with CuNPs for 10 days at concentrations of 40 and 100 mg l−1. Each experiment was conducted three times. To measure H_2O_2 a concentration, 100 mg of tissue was homogenized in an ice bath with 5 ml of 0.1% trichloroacetic acid (TCA), followed by centrifugation at 12,000 g for 15 minutes. The reaction mixture included 1 ml of 1M potassium iodide (KI) and 0.5 ml of 10 mM potassium phosphate buffer (pH 7.0). Absorbance was measured at 390 nm, and H_2O_2 content was quantified against a standard calibration curve, expressed as µM g−1 fresh weight. MDA, a byproduct of lipid peroxidation, was quantified via the thiobarbituric acid (TBA) test. The procedure involved homogenizing 100 mg of tissue in 5 ml of 0.1% TCA, centrifuging, and mixing 1 ml of 0.5% TBA in 20% TCA with 0.5 ml of the supernatant. After 30 minutes of boiling, the samples were cooled and centrifuged again. Absorbance was evaluated at 532 nm, adjusting for non-specific absorption at 600 nm, with the MDA-TBA complex concentration determined using an extinction coefficient of Ɛ = 155 mM−1 cm−1, also reported as µM g−1 fresh weight.

2.2.2 Assay of phenylalanine ammonia lyase (PAL) and antioxidant enzymes

The study examined the effects of CuNPs on the activities of phenylalanine ammonia-lyase (PAL) and antioxidant enzymes—catalase (CAT), ascorbate peroxidase (APX), and superoxide dismutase (SOD)- in fresh leaves and stems of control and BM plants treated with CuNPs at concentrations of 40 and 100 mg l-1 over 10 days.

To assess PAL activity, 1 g of fresh tissue was homogenized at 4°C with 5 ml of a 0.05 M Tris–HCl buffer (pH 8.0) containing 1% polyvinylpyrrolidone (PVP) and 0.8 mM β-mercaptoethanol. The mixture was centrifuged, and PAL activity was measured from the supernatant. For CAT, APX and SOD assays, an additional 1 g of plant material was homogenized in 3 ml of an extraction buffer comprising 50 mM Na_2PO_4, 1 mM EDTA, and 0.1% PVP (pH 7.0) at 4°C and subjected to centrifugation. The supernatant was preserved at -20°C for enzyme assays, with total protein concentration quantified using Bradfords method.

PAL activity was determined using a trans-cinnamic acid reaction mixture, which included Tris–HCl buffer, enzyme extract, phenylalanine, and distilled water. After one-hour incubation at 37°C, absorbance was measured at 290 nm. CAT activity was assessed by measuring the decrease in absorbance at 240 nm due to H_2O_2 decomposition in the presence of the enzyme extract. For APX activity, the reaction involved adding H_2O_2 to a mixture containing the enzyme extract and ascorbic acid; the decrease in absorbance at 290 nm was recorded. SOD activity was measured using the NBT technique, where the enzyme extract was mixed with various reagents and absorbance changes at 560 nm were monitored. Each enzyme activity was expressed in U mg−1 protein, indicating the efficacy of the enzymes under the experimental conditions. All experiments were repeated thrice for reliability [9], [10].

3. Result and Discussion

3.1 Synthesis of Ag and Cu nanoparticles

Waterlilies leaves extracts serve as reducing agents for synthesizing AgNPs and CuNPs, which are subsequently used as growth inducers for in vitro cultivation of *Bacopa monnieri* in Murashige and Skoog (1962) medium [4].

3.2 Characteristics of Ag and Cu nanoparticles:

Scanning Electron Microscope (SEM) with Energy Dispersive X-ray Analysis (EDAX) was utilized to assess the surface morphology and elemental composition of green synthesized nanoparticles (AgNPs and CuNPs). The morphology was found to range from 20 nm to 1 µm, shown in (Fig. 1-10). A well-distributed and non-agglomerated structure. EDAX confirmed the presence of elemental compositions including silver and copper oxide nanoparticles by displaying significant peaks for copper (Cu) and oxygen (O).

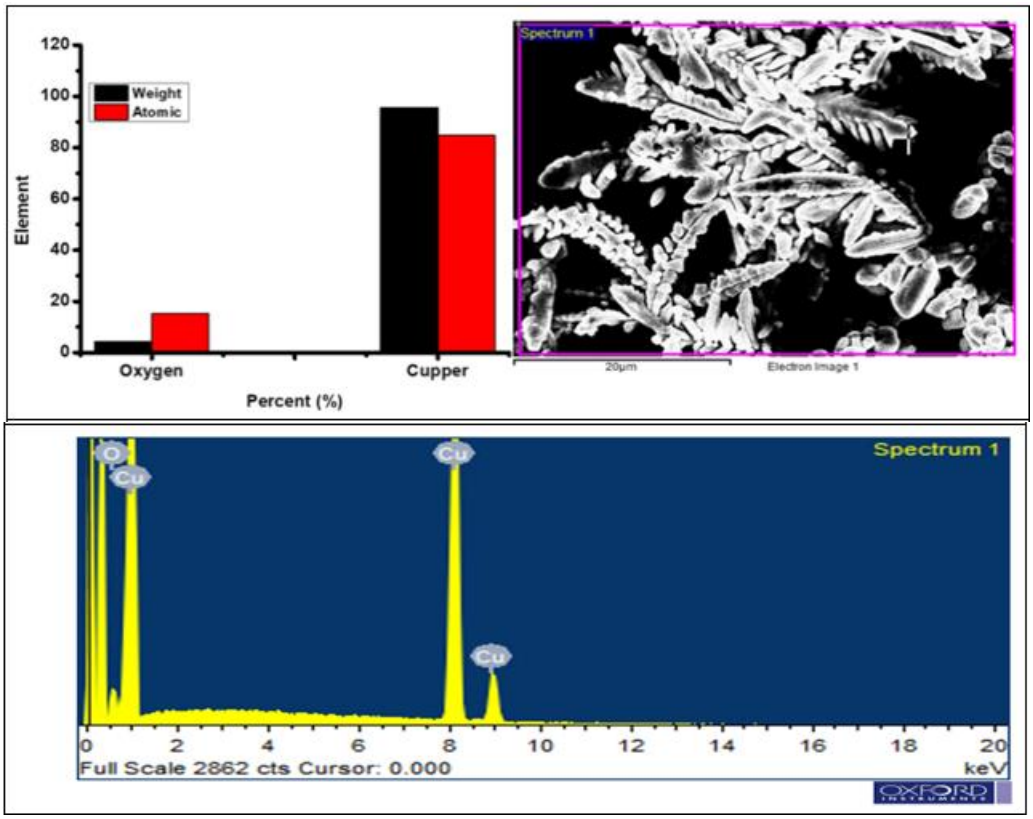

Figure 1: Weight and atomic percent in CuNPs sample and its SEM-EDX image.

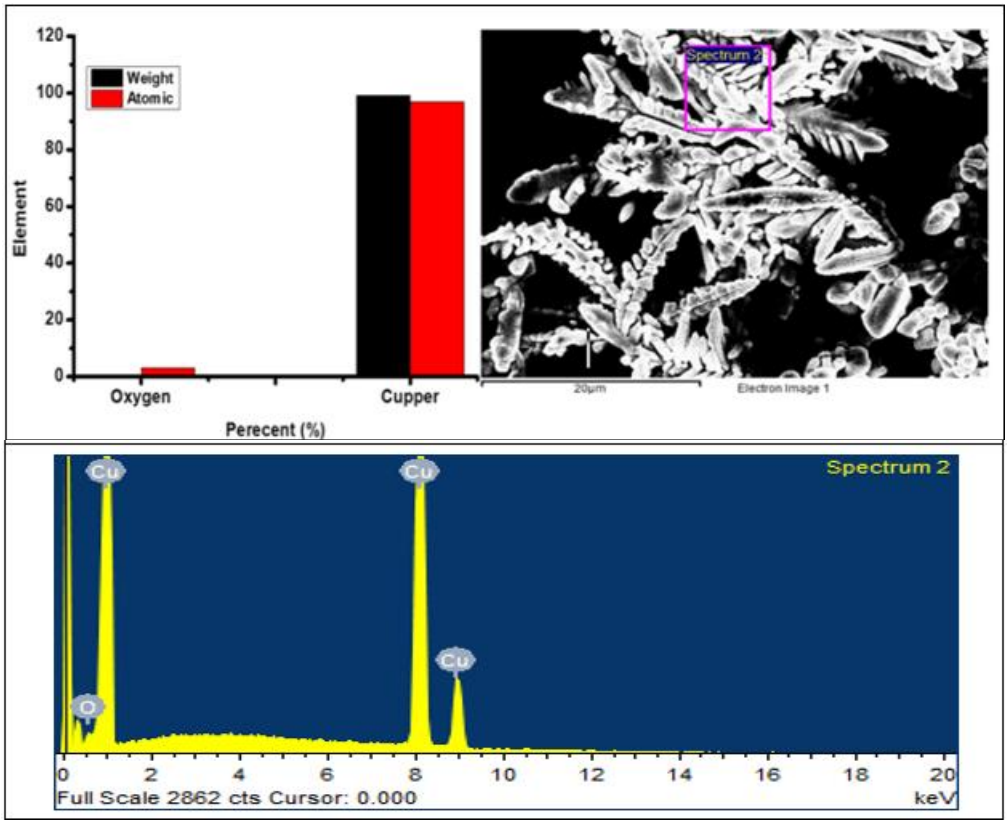

Figure 2: Weight and atomic present in CuNPs samples and its SEM-EDX image.

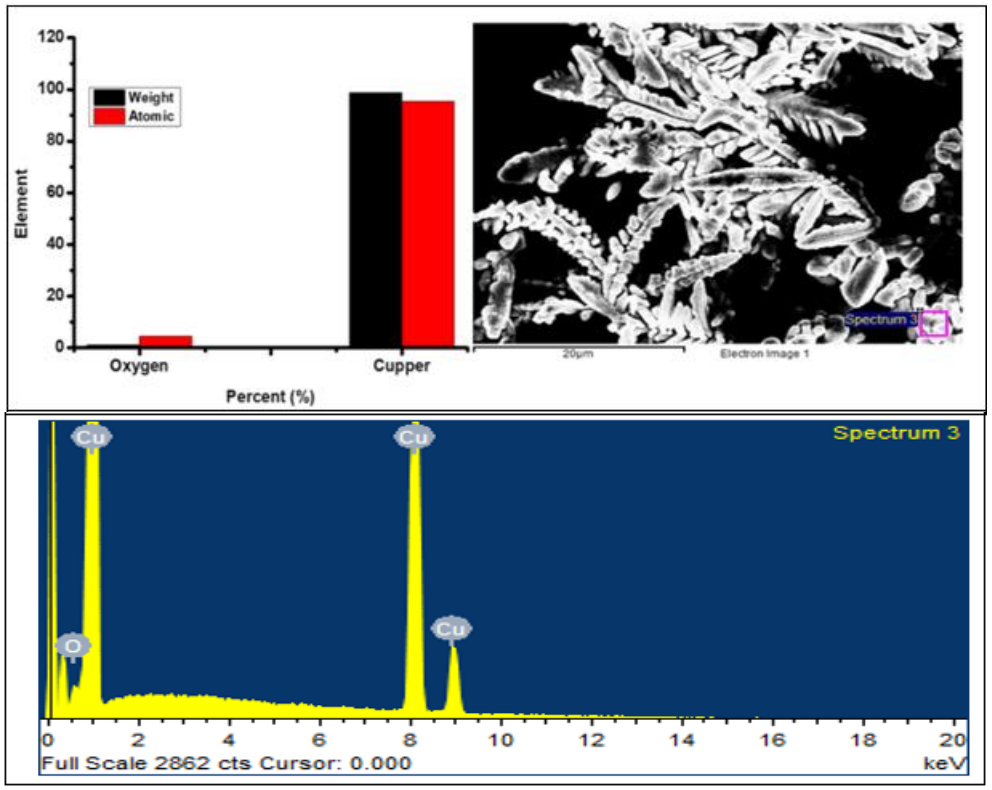

Figure 3: Weight and atomic percent of CuNPs sample and its SEM-EDX image.

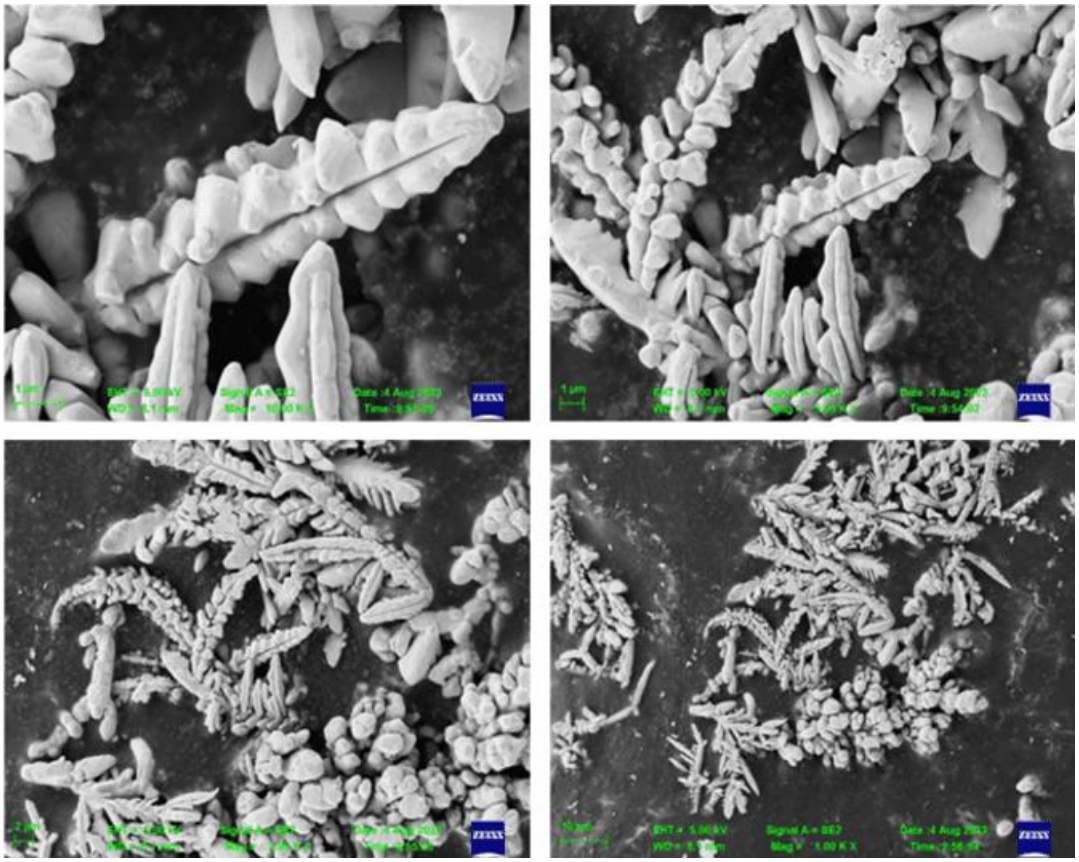

Figure 4: SEM image of CuNPs samples.

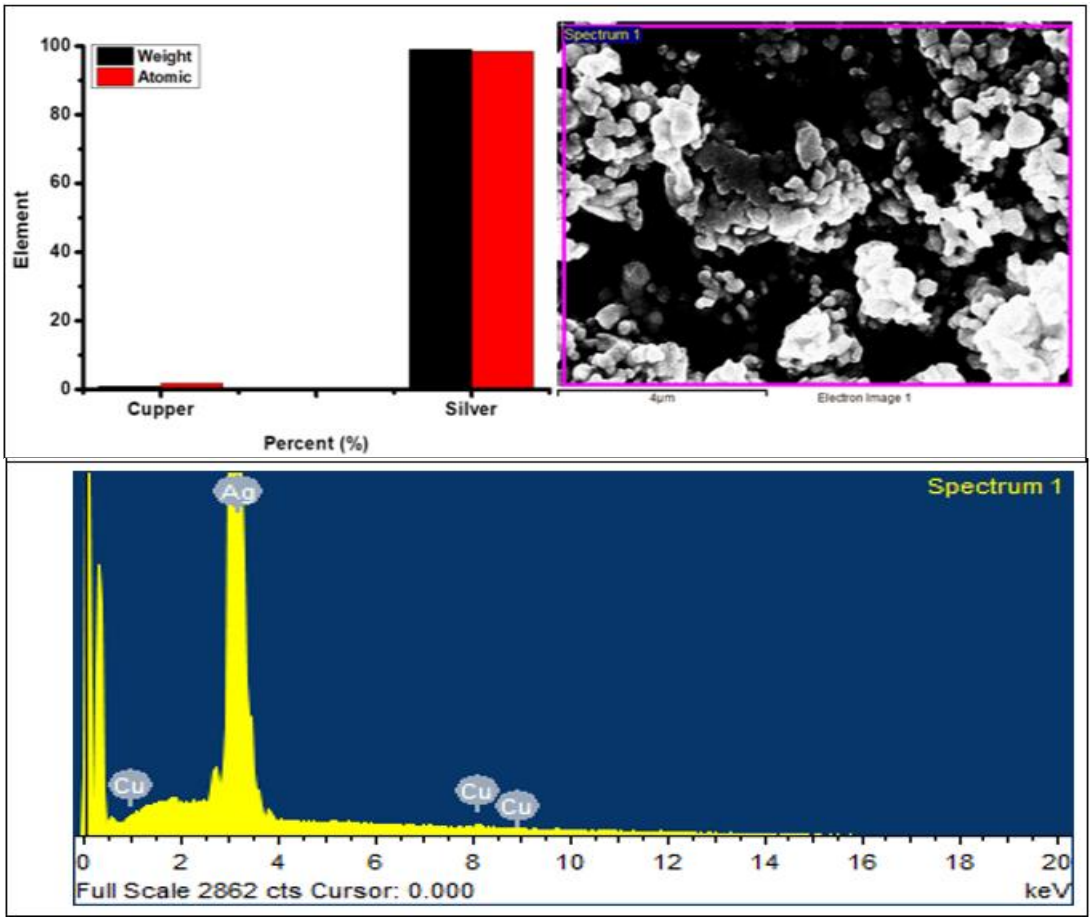

Figure 5: Weight and atomic percent of elements in AgNPs and its SEM image

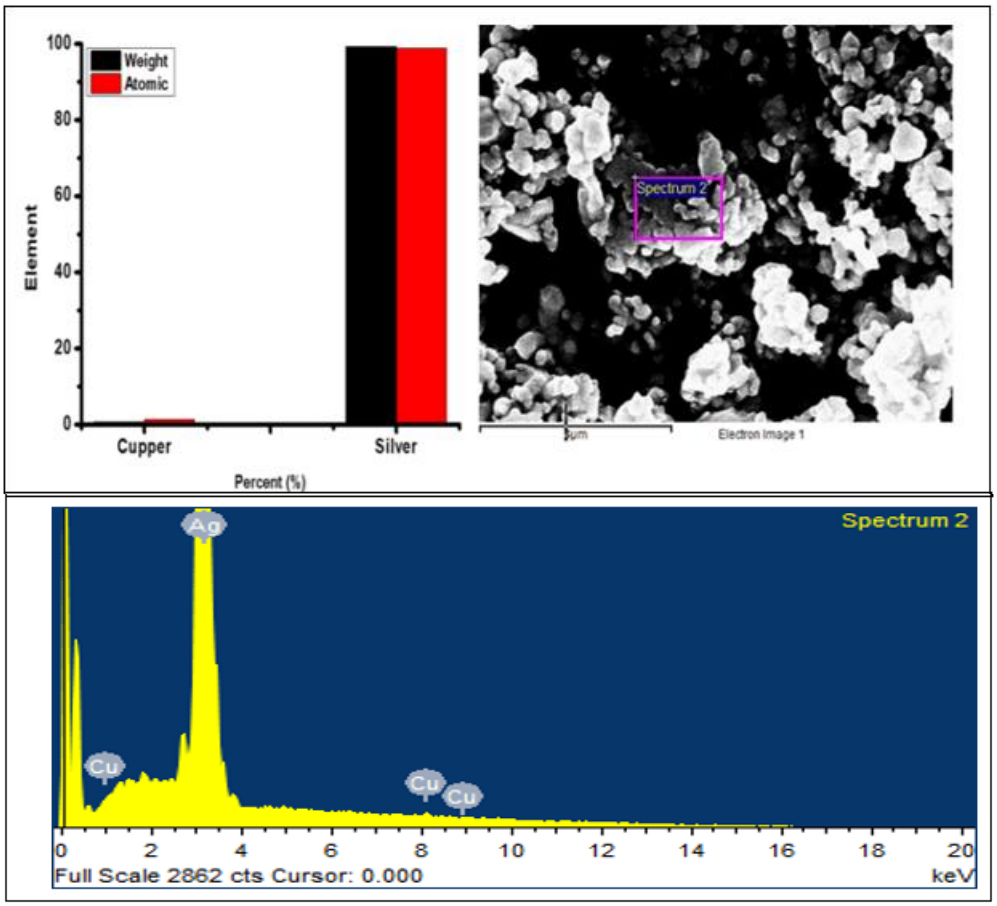

Figure 6: Weight and atomic percent of elements in AgNPs and its SEM image.

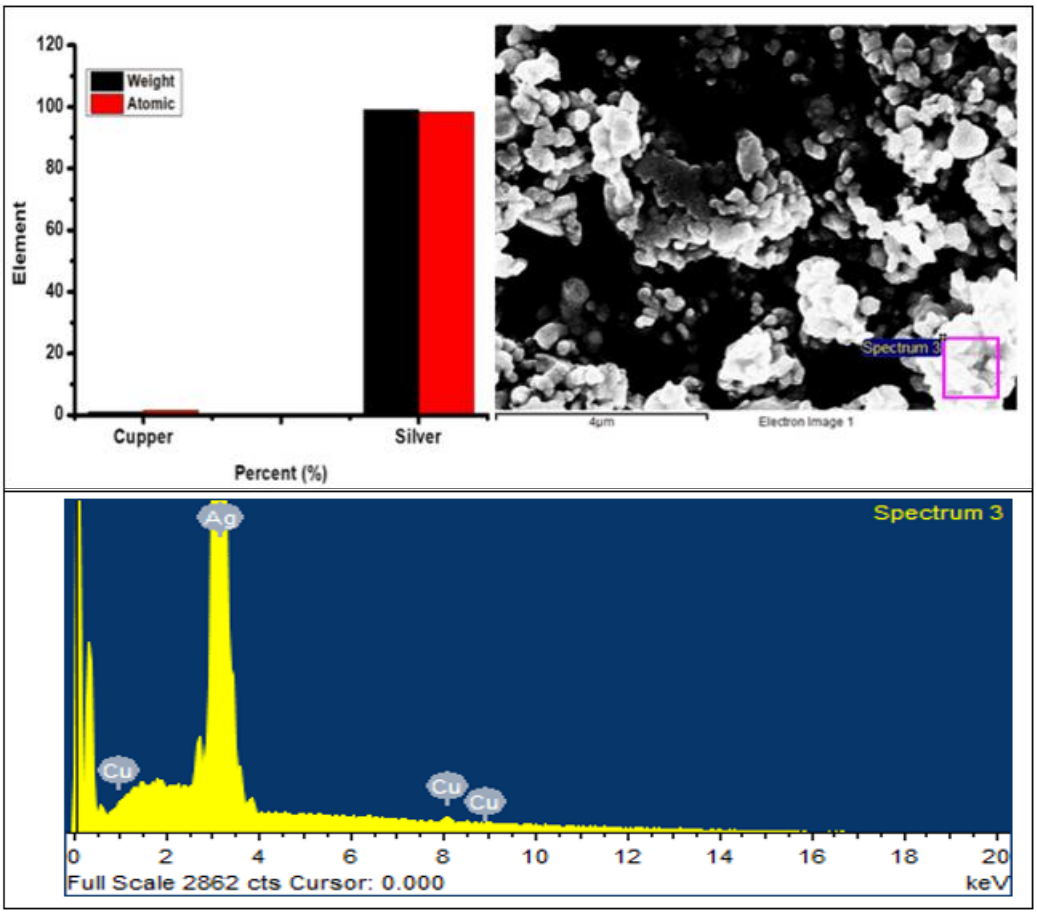

Figure 7: Weight and atomic percent of elements in AgNPs and its SEM image

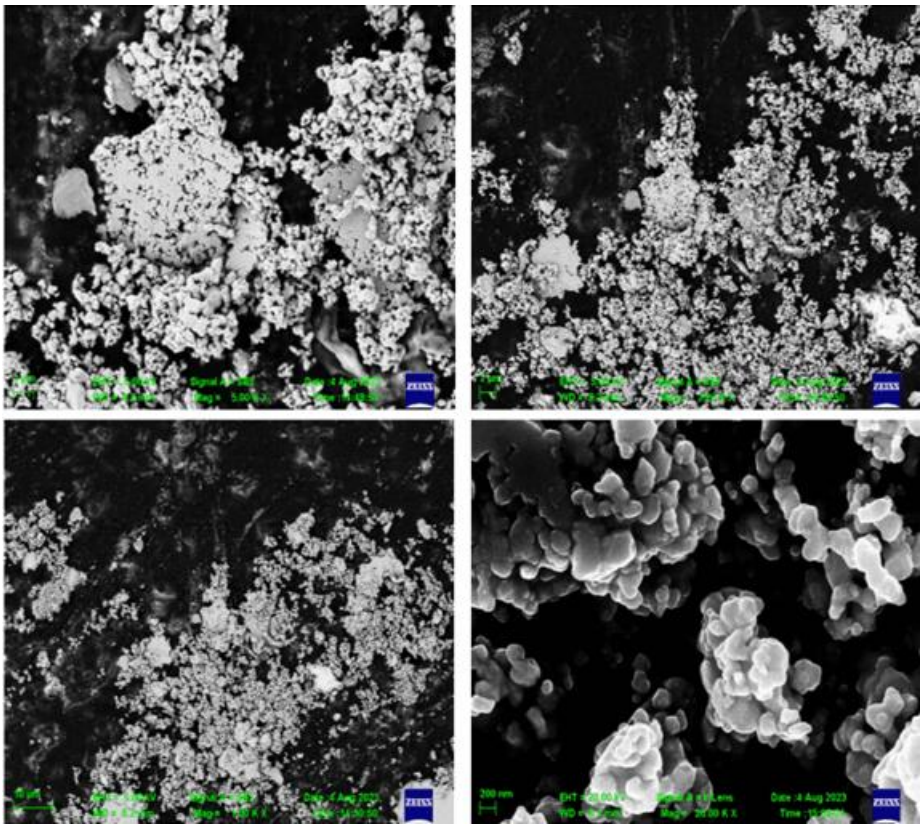

Figure 8: SEM image of AgNPs.

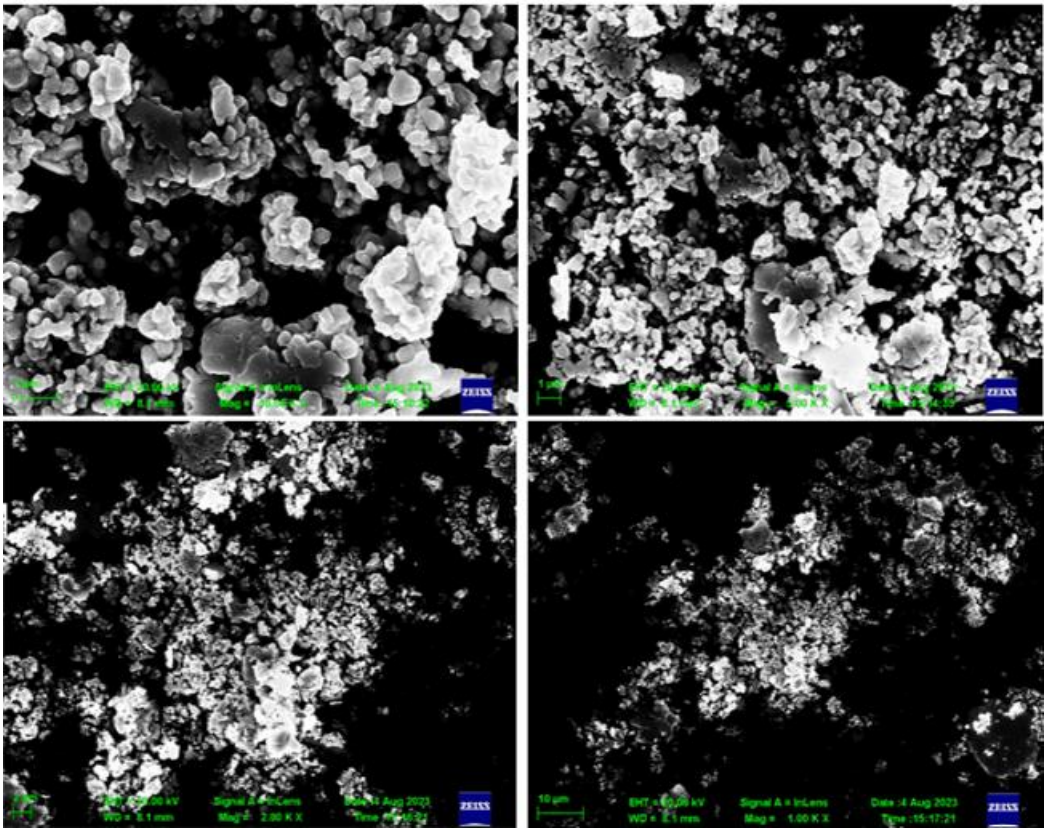

Figure 9: SEM image of AgNPs.

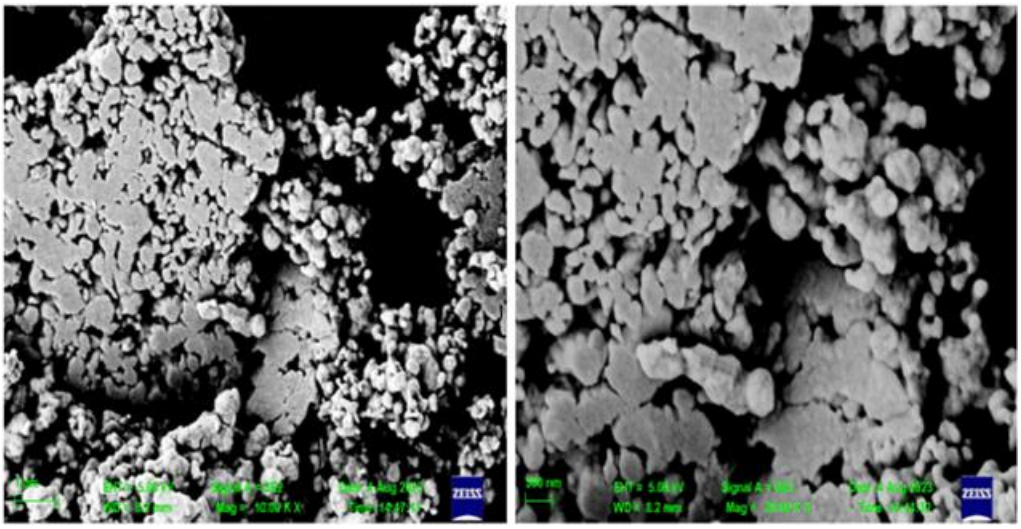

Figure 10: SEM image of AgNPs.

FTIR spectroscopy characterizes manufactured nanoparticles (AgNPs and CuNPs) and examines the relationship between their structure and properties. Synthesized from plant Waterlilis (Fig. 11,12), CuNPs exhibit maximum absorption at 3671.52 cm-1 and 1637.52 cm-1, while AgNPs show absorption at 2500 cm-1, 2000 cm-1, and 1700 cm-1.

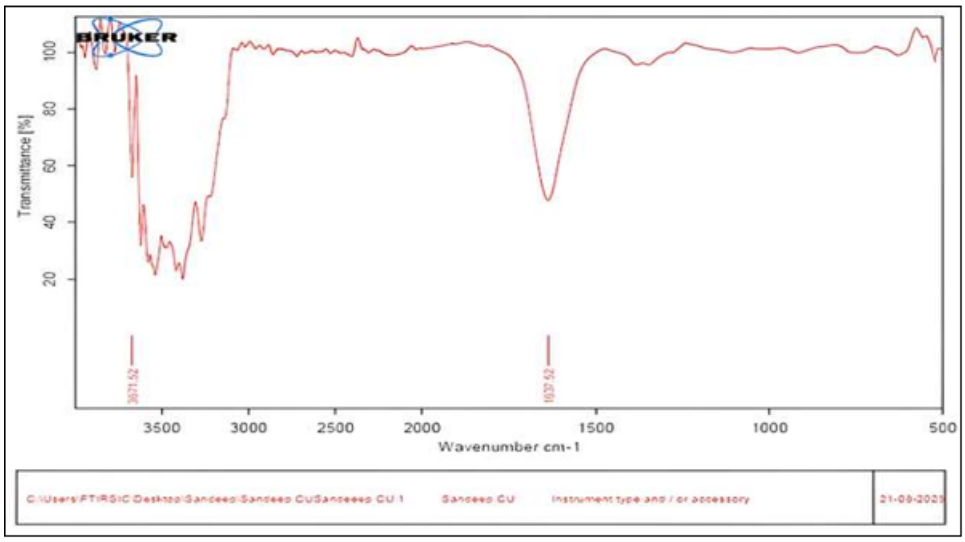

Figure 11: FTIR graph of CuNPs

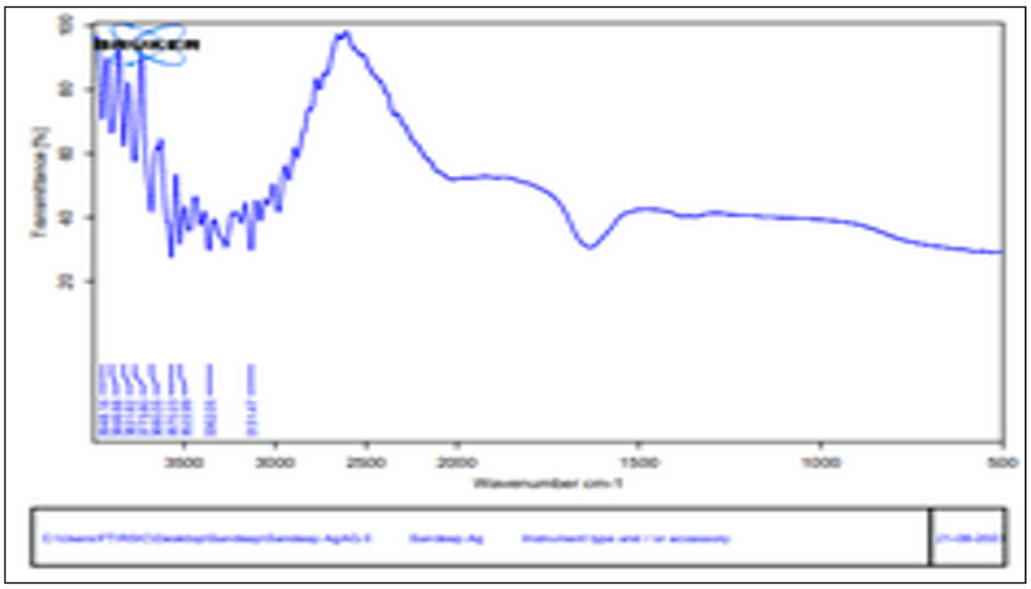

Figure 12: FTIR graph of AgNPs.

The crystalline size and composition of green synthesized AgNPs and CuNPs were analyzed using X-ray diffraction (XRD). (Fig. 12A and 12B) The results showed the nanoparticles had diffraction peaks corresponding to a monoclinic structure, with average crystallite sizes ranging from 1 to 100 nm, dependent on concentration. No contaminants were detected in the samples.

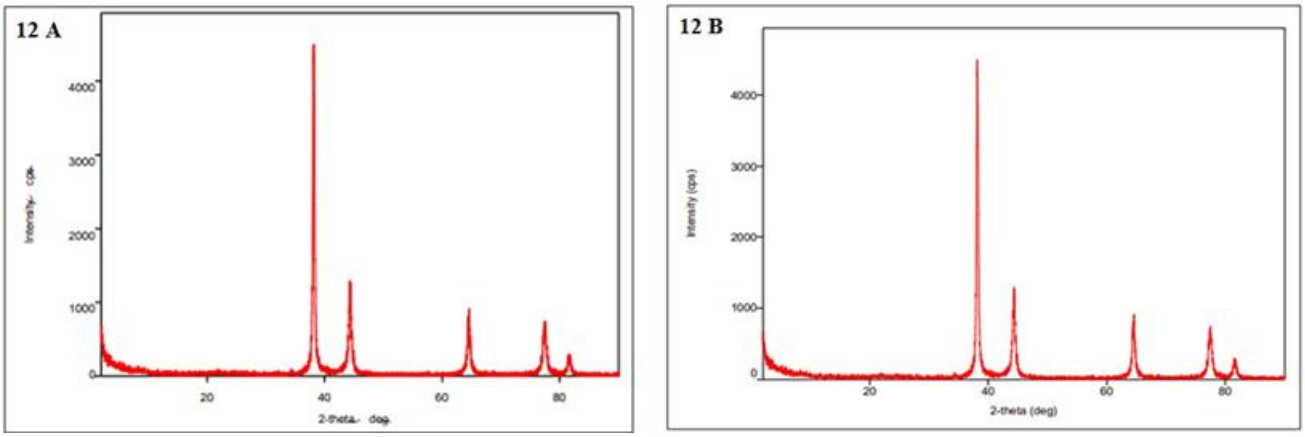

Figure 12: (A) XRD graph of CuNPs and (B) XRD graph of AgNPs.

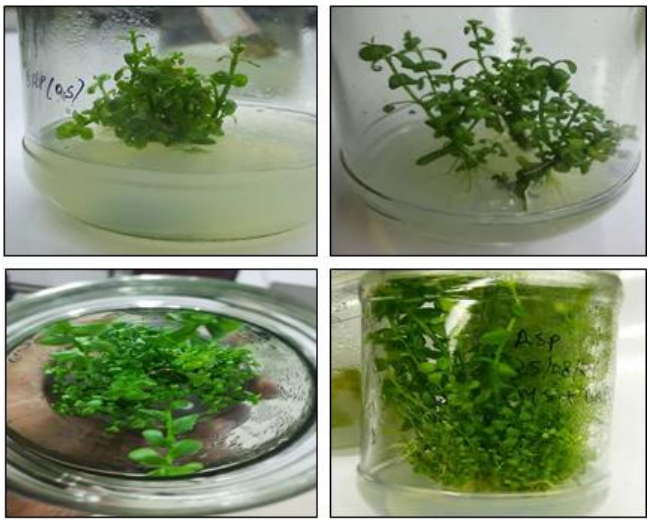

Figure 13: Shoot regeneration of *B. monneri L.*

Table 1: Morphogenic response of culture in MS medium with supplemented with different concentrations of cytokinins hypocotyl explants of *Baccopa monneri* L.

PGRs (mgL^{-1})	Mean frequency (%) of explants developing shoots	Mean number of shoots per explant
BAP		
Control	16	1.0 ± 0.1
0.5	30	2.4 ± 0.2
1	53	6.6 ± 0.5
2	43	5.6 ± 0.5
Kinetin		
Control	16	1.0 ± 0.1
0.5	23	1.5 ± 0.2
1	36	2.4 ± 0.3
2	30	2.0 ± 0.4
TDZ		
Control	16	1.0 ± 0.1
0.5	40	5.2 ± 0.4
1	60	8.0 ± 0.7
2	46	6.0 ± 0.4
Zeatin		
Control	16	1.0 ± 0.1
0.5	20	1.3 ± 0.2
1	26	1.7 ± 0.3
2	23	1.5 ± 0.4

Table 2: Influence of AgNPs on enhanced regeneration and biomass production in *Baccopamonneri* L.

AgNPs Concentration (µM)	MS medium supplemented with 1.0 mgL^{-1} TDZ	
	Mean frequency (%) of explants developing shoots	Mean number of shoots per explant
0	16	1.2± 0.1
10	46	6.2 ± 0.4
20	70	10.0 ± 0.8
30	50	4.0 ± 0.4
40	20	1.0 ± 0.1
50	10	1.0 ± 0.1
Cu NPs		
0	16	1.0 ± 0.2
10	33	1.5 ± 0.2
20	43	1.6 ± 0.2
30	40	1.4 ± 0.2
40	10	1.0 ± 0.1
50	0	0.0 ± 0.0

3.3 Effect of cytokinis alone on shoots regeneration

In the context of cytokinin effects, TDZ is notably effective for direct shoot regeneration, inducing shoot formation across all tested concentrations. Table:2 shows comparatively; other cytokinins like BAP, kinetin and zeatin exhibited varying degrees of shoot development from hypocotyl explants, with zeatin being less effective at lower concentrations. TDZs impact on shoot regeneration is consistent across 0-2 mg/L concentrations, but an increase to 2 mg/L results in decreased regeneration. Overall, TDZ alone proves to be more effective than the other cytokinins, whether used independently or in combination with auxins.

3.4 Effect of AgNPs and CuNPs on secondary metabolism of *B. monnieri*

Exposure to AgNPs and CuNPs significantly increased total saponin and alkaloid content in *Bacopa monnieri* compared to controls (Figure 14). At various concentrations, CuNPs consistently demonstrated a stronger enhancement effect than AgNPs. At 10 mg/L, saponin levels were ~20 mg/g DW for AgNPs, while CuNPs reached ~33 mg/g DW, indicating a 65% higher accumulation with CuNPs. This trend continued across all tested concentrations, with CuNPs peaking at 45 mg/g DW at 40 mg/L, while AgNPs maxed out at 30 mg/g DW. For alkaloids, both types of nanoparticles increased content progressively, with CuNPs again maintaining a higher level at all concentrations, showing greater elicitation of alkaloid biosynthesis in *B. monnieri* compared to AgNPs. Maximum alkaloid levels were recorded at 50 mg/L, further affirming the superior efficacy of CuNPs over AgNPs (Figure 15).

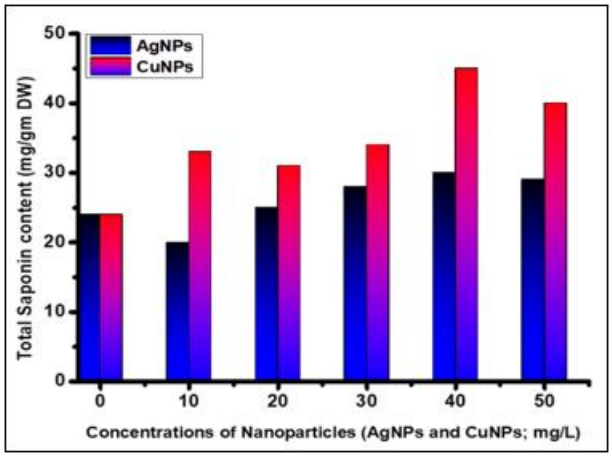

Figure 14: Total saponin content after exposure of AgNPS and CuNPs on *B. monneri* L.

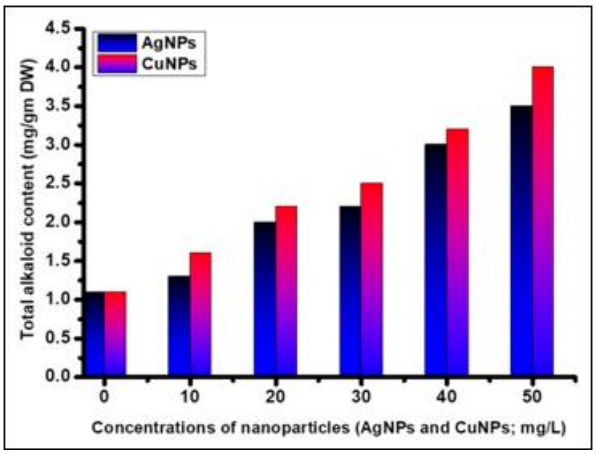

Figure 15: Alkaloid content after exposure of AgNPS and CuNPs on *B. monneri* L.

The total phenolic content in *Bacopa monnieri* increased with dosage from AgNPs and CuNPs up to 30 mg/L, after which it declined at higher concentrations (40–50 mg/L). CuNPs consistently led to higher phenolic accumulation than AgNPs throughout all treatments. At the baseline (0 mg/L), phenolic content was low, with CuNPs slightly higher than AgNPs. Both nanoparticles boosted phenolic levels at 10 and 20 mg/L, with CuNPs showing greater increases. The peak accumulation occurred at 30 mg/L, predominantly driven by CuNPs. At 40 mg/L, phenolic content declined but remained higher under CuNP treatment, and a slight rise was noted at 50 mg/L, with CuNPs still outperforming AgNPs (Figure 16).

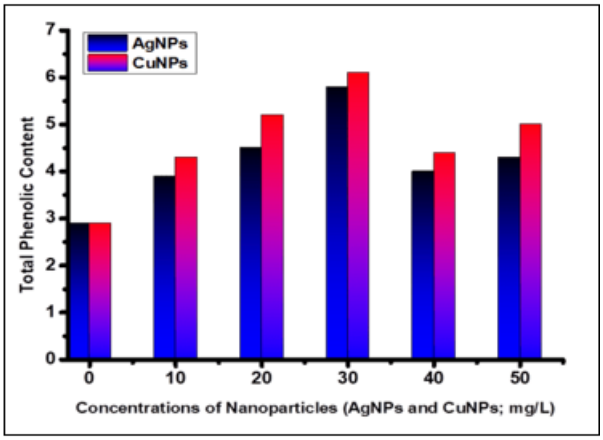

Figure 16: Total phenolic content after exposure of AgNPS and CuNPs on *B. monneri* L

The study demonstrates that the total flavonoid content in *Bacopa monnieri* increased with higher concentrations of both silver nanoparticles (AgNPs) and copper nanoparticles (CuNPs) up to 50 mg/L. CuNPs consistently resulted in a greater accumulation of flavonoids than AgNPs at all tested concentrations. CuNPs showed significant enhancement at 0 mg/L, 10 mg/L, and continued to outperform AgNPs at 20 mg/L, 30 mg/L, and 40 mg/L. The maximum flavonoid content was observed at 50 mg/L, with CuNPs leading to the highest levels compared to AgNPs (Figure 17).

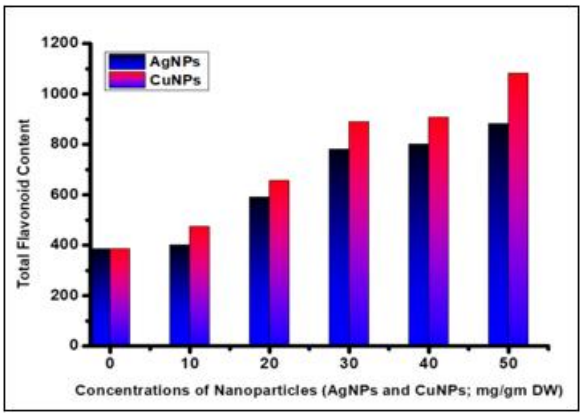

Figure 17: Total flavonoid content after exposure of AgNPs and CuNPs on *B.monneri* L.

3.5 Effect of CuNPs on hydrogen peroxide and MDA contents of *B. monnieri*

Exposure of *Bacopa monnieri* shoots to AgNPs and CuNPs led to a concentration-dependent increase in oxidative stress indicators, namely hydrogen peroxide (H_2O_2) and malondialdehyde (MDA). The rising levels of H_2O_2 and MDA signify that CuNPs primarily induce oxidative stress through increased reactive oxygen species (ROS) production, particularly H_2O_2, which is significant due to its capability to penetrate cellular membranes and serve as a signaling molecule in plant stress responses. Enhanced MDA levels reflect lipid peroxidation and membrane damage due to oxidative stress.

While copper is a vital micronutrient for various enzymatic functions, its nanoparticle form can disrupt redox balance. Prior studies have indicated that CuO nanoparticles hinder the electron transport chain in *Nicotiana tabacum* BY-2 cells, resulting in elevated ROS, including H_2O_2 and hydroxyl radicals, which damage membranes evidenced by increased MDA and lactate dehydrogenase activity. Similar oxidative damage from CuNPs has been documented in multiple plant species, which corroborates the current findings that CuNPs have a significant oxidative effect, leading to heightened ROS levels and increased lipid peroxidation in *Bacopa monnieri* [11], [12].

3.6 Effect of AgNPs and CuNPs on PAL and anti-oxidant enzymes of *B. monnieri*

AgNPs and CuNPs enhance the levels of PAL, CAT, APX, and SOD in *B. monnieri*. At a concentration of 40 mg l−1, increases were approximately 91% for PAL, 90% for CAT, 147% for APX and 117% for SOD in leaves, and 88%, 95%, 122%, and 95% in stems, respectively. These levels dropped to near control levels at 100 mg l−1. The action of CuNPs mirrors that of AgNPs, suggesting the activation of antioxidant defense and secondary metabolism through ROS production. PAL is key in the phenylpropanoid pathway, converting phenylalanine to cinnamic acid, linking primary metabolism to secondary metabolisms aromatic amino acids. Elevated ROS from CuNPs activate both enzymatic and non-enzymatic antioxidant defenses across multiple species.

Many plant species, including *Brassica napus*, *Brassica juncea*, *Cucumis sativus*, *Oryza sativa* and others, have been

shown to activate antioxidant enzymes such as catalase (CAT), ascorbate peroxidase (APX), and superoxide dismutase (SOD) when exposed to copper (CuNPs) and silver nanoparticles (AgNPs). Specific studies report that doses of 10 mg and 100 mg of $Cu(OH)_2$ nanopesticide significantly enhance the expression of antioxidant enzyme genes like POD1 and GST1 in Zea mays. CAT dismutates hydrogen peroxide (H_2O_2) into water and oxygen, while SOD converts superoxide into H_2O_2, with APX playing a key role in the ascorbate-glutathione cycle by reducing H_2O_2 to water. An inhibition of enzyme synthesis or issues with enzyme subunit assembly is identified as a general stress response, resulting in decreased enzyme content at toxic levels [13], [14].

Plant enzyme activity is negatively impacted by heavy metal stress, leading to cell membrane oxidative damage. Copper-based nanoparticles are particularly phytotoxic due to their release of ions and excess reactive oxygen species (ROS). This overproduction of ROS can result in DNA damage, lipid peroxidation, apoptosis, and protein structure breakdown. However, plants possess enzymatic systems, including catalase (CAT), peroxidase (POD), ascorbate peroxidase (APX), and superoxide dismutase (SOD), which help mitigate the harmful effects of ROS and protect biomolecules from oxidative damage [15], [17].

CuNPs induce the production of reactive oxygen species (ROS) in plants like *B. monnieri*, activating both antioxidant defenses and secondary metabolic pathways. This is evidenced by increased levels of H_2O_2 and MDA, and elevated activities of antioxidant enzymes such as CAT, APX and SOD. However, metallic CuNPs tend to oxidize into Cu_2O or CuONPs, which can negatively affect plants, with intracellular nanoparticles causing long-term toxicity and dissolved Cu2+ ions leading to acute effects. CuONP exposure has been shown to upregulate 47 oxidative stress genes in Arabidopsis thaliana.
Studies indicate that silver nanoparticles (AgNPs) can accumulate in plants and impact stress responses. Qian et al. (2013) found that AgNPs altered the transcription of antioxidant and aquaporin genes in Arabidopsis, affecting the oxidant-antioxidant balance. De La Torre-Roche et al. (2013) reported that soybean exposed to high AgNP concentrations led to a significant increase in malondialdehyde (MDA), highlighting lipid peroxidation under stress. Thiruvengadam et al. (2015) observed that higher AgNP exposure in turnip seedlings resulted in increased lipid peroxidation and superoxide radical production, with notable hydrogen peroxide (H_2O_2) generation at lower concentrations [19], [20].

The DPPH radical scavenging capacity of *Bacopa monnieri* increased with higher concentrations of AgNPs and CuNPs (0–50 mg/L). CuNP-treated shoots consistently showed greater antioxidant activity than AgNPs at all concentrations. Both nanoparticles had baseline activity at 0 mg/L, but significant increases were noted at 10 mg/L, with CuNPs slightly outperforming AgNPs. At 20 mg/L, CuNPs distinctly exceeded AgNPs in scavenging capacity, and this trend continued at 30 and 40 mg/L, culminating in maximum activity at 50 mg/L (Figure 18). The results demonstrated that CuNPs effectively enhance the DPPH scavenging ability and indicate a dose-dependent increase in antioxidant activity, suggesting that CuNPs stimulate stronger antioxidant mechanisms in *B. monnieri* compared to AgNPs.

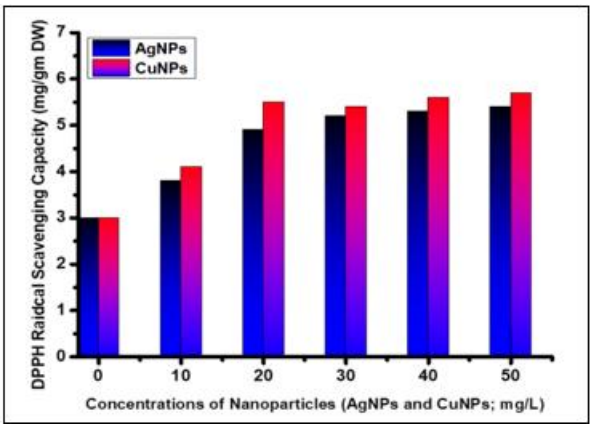

Figure 18: DPPH radical scavenging capacity after exposure of AgNPS and CuNPs on *B. monneri L.*

The study found that *Bacopamonnieri* exposed to AgNPs showed a significant increase in bacoside content, rising from a baseline of ~20 mg/g DW to ~28 mg/g DW. In contrast, CuNPs led to a slight elevation in bacosides (~19–20 mg/g DW), which was lower than the control and AgNP-treated levels (Figure 19). This indicates that AgNPs are more effective in eliciting bacoside biosynthesis, likely through the activation of metabolic pathways via oxidative signaling. This aligns with previous findings of nanoparticle-mediated enhancements in bioactive metabolites in medicinal plants.

In contrast to CuNPs, which induce lower bacoside levels due to higher oxidative stress that disrupts normal metabolism, AgNPs enhance bacoside accumulation more effectively. CuNPs elevate ROS levels, diverting metabolic energy away from secondary metabolite production, impacting species like Coriandrum sativum and Oryza sativa. Conversely, AgNPs have been shown to increase saponin and phenolic accumulation in Panax ginseng and Withania somnifera, likely due to the activation of defense-related transcription factors or key enzymes, promoting triterpenoid biosynthesis. Thus, AgNPs provide a controlled ROS signaling that avoids excessive oxidative damage [21].

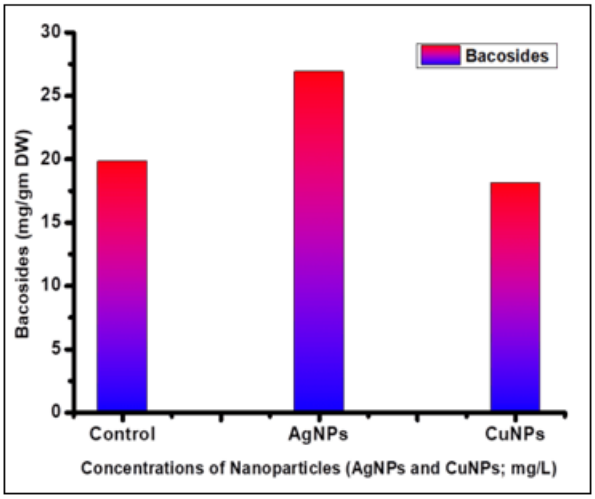

Figure 19: Bacosides (mg/g, DW) content after exposure of AgNPS and CuNPs on B. *monneri* L.

The study indicates that hydrogen peroxide (H_2O_2) levels in *Bacopamonnieri* L. increased with higher concentrations of CuNPs, demonstrating a marked dose-dependent response, while AgNPs showed no effect on H_2O_2 accumulation. At 10 mg L^{-1} of CuNPs, H_2O_2 reached approximately 6 µg g^{-1} FW, increasing to nearly 16 µg g^{-1} FW at 50 mg L^{-1} (Figure 20). The findings suggest that CuNPs induce oxidative stress due to their capacity to generate reactive oxygen species (ROS), aligning with prior research on Cu-based nanoparticles. In contrast, AgNPs may be more tolerated by *B. monnieri* or less reactive, as they did not produce measurable H_2O_2 levels, possibly reflecting their lower reactivity and varying effects across different plant species [22], [23]. Overall, CuNPs demonstrated a strong elicitor or stress-inducing effect, whereas AgNPs exhibited negligible oxidative influence on *B. monnieri*, highlighting the differential physiological responses of plants to chemically distinct nanoparticles.

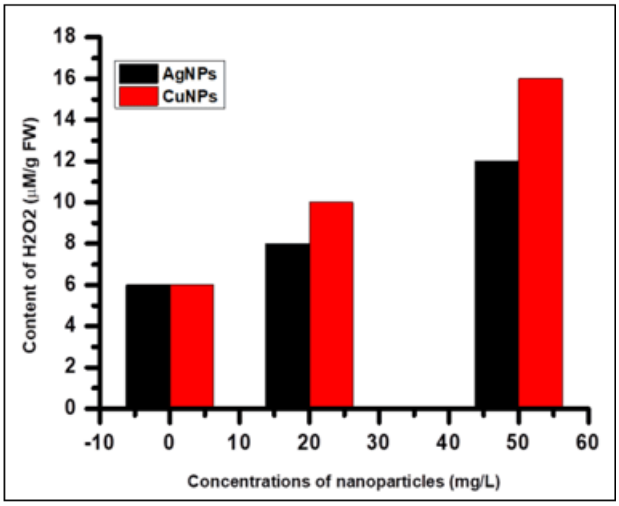

Figure 20: Content of H_2O_2 after exposure of AgNPS and CuNPs on *B. monneri* L.

The study investigates the effects of AgNPs and CuNPs on malondialdehyde (MDA) content in *Bacopa monnieri* L. Findings indicate that MDA levels significantly increased with rising concentrations of CuNPs, with values reaching 0.8 µmol g^{-1} FW at 50 mg L^{-1}, highlighting severe lipid peroxidation and oxidative membrane damage. In contrast, AgNPs showed no detectable MDA accumulation, indicating they did not induce oxidative stress in the plant (Figure 21). Overall, the results underscore that CuNPs can severely disrupt membrane stability in *B. monnieri*, while AgNPs appear benign in this context, as demonstrated by the absence of MDA accumulation across all concentrations tested.

CuNPs are known to generate reactive oxygen species (ROS), leading to oxidative damage in lipids and biomolecules, with higher concentrations exacerbating toxicity as evidenced by increased MDA formation. This concentration-dependent effect has been observed in various plant systems. Conversely, AgNPs do not appear to induce ROS in *B. monnieri*, suggesting that either ROS production is minimal or the plant effectively manages oxidative stress. Studies indicate that AgNPs may have a less significant impact on membrane lipid stability compared to CuNPs, showing milder physiological responses at low to moderate doses [24], [25].

The differential responses to AgNPs and CuNPs suggest that CuNPs pose a greater oxidative risk, while AgNPs appear less damaging to membrane integrity in *B. monnieri* under the tested conditions.

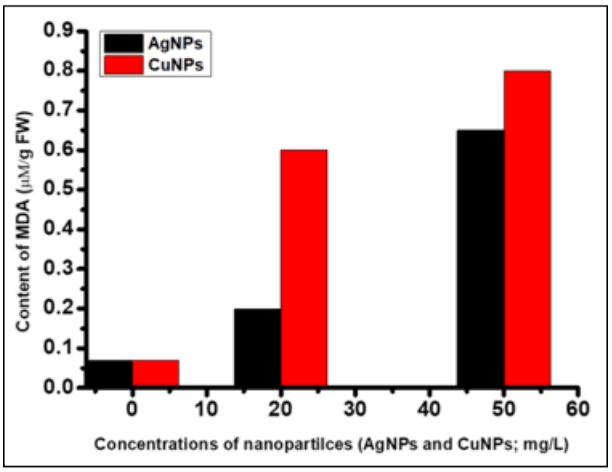

Figure 21: Content of MDA after exposure of AgNPS and CuNPs on *B. monneri* L.

The study indicates that CuNPs significantly enhance phenylalanine ammonia-lyase (PAL) activity in *Bacopa monnieri*, with increased activity noted at concentrations up to 20 mg/L, peaking at approximately 2.0 U g^{-1} FW. At a higher concentration of 60 mg/L, PAL levels slightly declined to 1.5 U g^{-1} FW, yet remained significantly above control levels. Conversely, AgNPs did not induce any detectable PAL activity across all tested concentrations (10–60 mg/L), indicating no stimulatory effect on the PAL pathway (Figure 22). PAL is a crucial enzyme in the phenylpropanoid pathway, often activated by abiotic stressors and nanoparticle exposure [26]. The results underscore the strong elicitation potential of CuNPs compared to the negligible effect of AgNPs. CuNPs are also identified as moderate inducers of oxidative stress, stimulating reactive oxygen species (ROS) that activate indeed PAL and enhance phenolic metabolism across various plant species. Prior studies have corroborated the role of CuNPs in boosting phenolic accumulation and PAL activity in plants like *Ocimum sanctum* and *Salvia officinalis* through ROS-mediated signaling. The observed rise in PAL activity at an optimal 20 mg/L concentration of CuNPs signifies a threshold for effective stress induction, beyond which, at 60 mg/L, the slight decrease in activity may suggest onset of stress saturation or toxicity.

The absence of phenylalanine ammonia-lyase (PAL) activity in *B. monnieri* following AgNPs exposure indicates that these nanoparticles are not recognized as elicitors for phenylpropanoid metabolism. Instead, they may have direct cytotoxic effects, inhibit metabolic enzyme activation, and produce lower reactive oxygen species (ROS) levels, insufficient to trigger defense mechanisms. Conversely, CuNPs enhance PAL activity, promoting phenolic and flavonoid synthesis, thereby improving antioxidant capacity and medicinal value, signifying significant metabolic reprogramming.

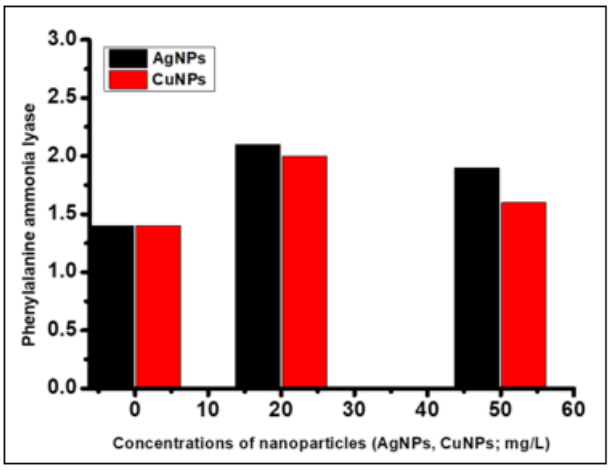

Figure 22: Phenylalanine amnonia-lyase content after exposure of AgNPS and CuNPs on *B. monneri* L.

The study reveals that CuNPs significantly enhance catalase (CAT) activity in *Bacopa monnieri*, with peak activity at 20 mg/L reaching ~100 U mg^{-1} TP. At 10 mg/L, activity was ~78 U mg^{-1} TP, and though it decreased to ~82 U mg^{-1} TP at 60 mg/L, it remained above control levels. In contrast, AgNPs did not stimulate CAT activity, showing values near zero across concentrations. CuNPs act as metabolic elicitors, inducing antioxidant defense mechanisms by generating controlled reactive oxygen species (ROS) that activate enzyme pathways. The results align with previous studies indicating that Cu-based nanoparticles can upregulate antioxidant enzymes and enhance oxidative resilience in plants. The decline in CAT activity at higher concentrations suggests potential oxidative toxicity from excessive Cu exposure. Lack of catalase (CAT) induction under AgNPs is noted, unlike CuNPs, which enhance CAT activity (Figure 23). Possible explanations for AgNPs ineffectiveness include interference with antioxidant enzyme synthesis, increased cytotoxicity, inadequate reactive oxygen species (ROS) signalling for CAT expression or enzyme inactivation by silver ions. Studies indicate that AgNPs can have species-dependent inhibitory effects, suppressing enzyme activity due to nanoparticle-induced damage or altered redox regulation. The stress induced by excess AgNPs may surpass the plant's capacity to activate CAT, particularly in sensitive medicinal herbs, suggesting an inhibitory effect in *B. monnieri* [26].

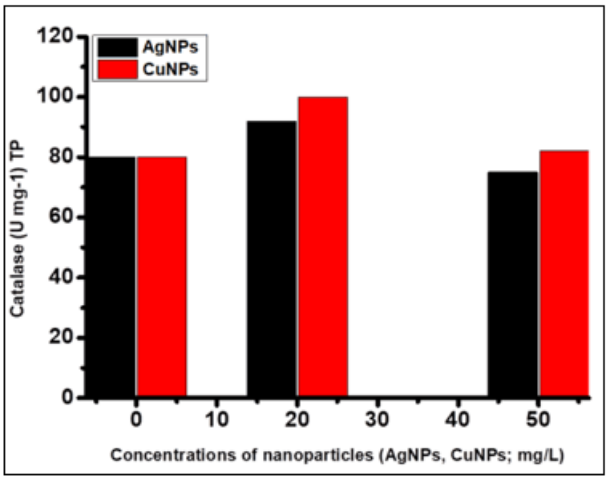

Figure 23: Catalase content after exposure of AgNPS and CuNPs on *B. monneri* L.

The ascorbate peroxidase (APX) activity in *Bacopa monnieri* demonstrated a notable differential response to CuNPs and AgNPs. APX activity significantly increased with CuNPs treatment, peaking at 20 mg/L (approximately 3.2 U mg^{-1} TP), while AgNPs showed no measurable activity at any concentration. A slight decrease in APX activity occurred at 60 mg/L CuNPs (around 2.0 U mg^{-1} TP), but it remained above control levels (Figure 24). The results indicate that CuNPs notably activate the ascorbate–glutathione detoxification pathway and suggest their role as effective elicitors of reactive oxygen species (ROS)-mediated defense mechanisms, contrasting with AgNPs, which do not stimulate the antioxidant defense system in *B. monnieri.*

This response indicates that *B. monnieri* views CuNPs as metabolic stimulants, enhancing H_2O_2 detoxification through the ascorbate–glutathione cycle. Similar findings in previous studies highlight CuNPs ability to boost antioxidant activity and phenolic metabolism due to controlled ROS signaling. Conversely, AgNP treatments do not activate APX, likely due to their more severe cytotoxic effects, which inhibit antioxidative enzymes by disrupting thiol groups and redox-sensitive signaling pathways. The lack of APX activity suggests that AgNPs either fail to produce necessary ROS signals for enzyme induction or negatively impact antioxidant enzyme synthesis and stability in *B. monnieri*, consistent with findings in other medicinal plants [26], [27].

Overall, CuNPs significantly enhance APX activity in *Bacopa monnieri*, boosting its antioxidant defense, while AgNPs do not affect the ascorbate–glutathione pathway. CuNPs show potential as elicitors for improving oxidative stress tolerance and secondary metabolite biosynthesis.

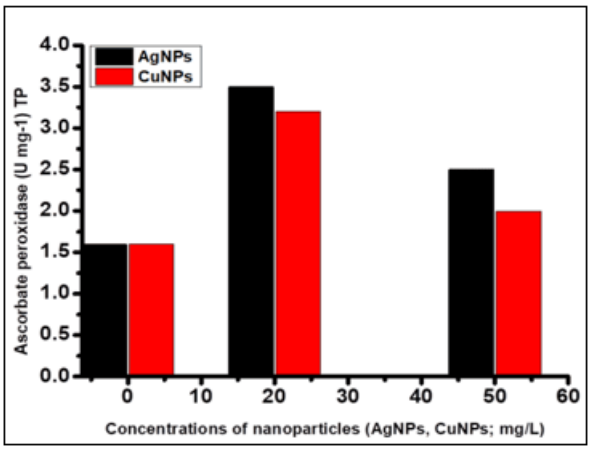

Figure 24: Ascorbate peroxidase content after exposure of AgNPS and CuNPs on *B. monneri* L.

Exposure to AgNPs and CuNPs in *Bacopamonnieri* elicited distinct physiological responses, highlighting differential oxidative stress modulation. Both nanoparticles caused a progressive increase in hydrogen peroxide (H_2O_2), with CuNPs inducing a more significant accumulation, particularly at 60 mg/L, suggesting stronger oxidative signaling. In contrast, AgNPs resulted in lower H_2O_2 levels. Lipid peroxidation, indicated by malondialdehyde (MDA) content, rose under both treatments, with CuNPs causing sharper increases at higher concentrations (40–60 mg/L), reflecting greater membrane damage. AgNPs produced moderate MDA accumulation, indicating lesser oxidative toxicity (Figure 25).

These results demonstrate that while both nanoparticles induce oxidative stress, CuNPs have a stronger pro-oxidant effect.

Superoxide dismutase (SOD) activity revealed significant differences between AgNPs and CuNPs. AgNPs did not activate SOD, indicating potential inhibition of the ROS-scavenging mechanism. In contrast, CuNPs significantly induced SOD activity in a concentration-dependent manner, peaking at 20 mg/L, suggesting an effective antioxidant response against superoxide radicals. Additionally, CuNPs increased saponin accumulation, especially between 20-40 mg/L, supporting the idea that controlled oxidative signaling enhances secondary metabolite biosynthesis. AgNPs showed minimal impact on saponin levels and lacked induction of ROS-signaling pathways, suggesting cytotoxic effects. Overall, CuNPs effectively elicit antioxidant defenses and metabolite production, while AgNPs appear more toxic, inhibiting enzymatic activity and disrupting ROS balance, making CuNPs a better choice for elicitation in *Bacopamonnieri*.

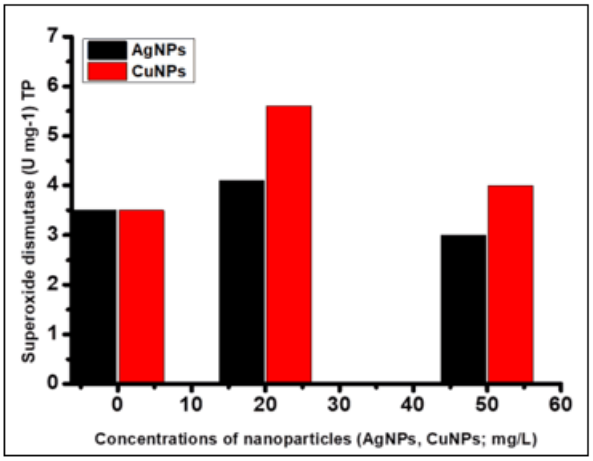

Figure 25: Superoxide dismutase content after exposure of AgNPs and CuNPs on *B. monneri* L.

4. Conclusion

Green synthesis of AgNPs and CuNPs using Waterlily leaf extracts was successfully achieved, and their characterization confirmed nanoscale size, uniform morphology, monoclinic crystalline structure, and purity. SEM, EDAX, FTIR, and XRD analyses validated their structural and elemental properties, making them suitable as bioactive elicitors.

In vitro studies on *Bacopa monnieri* demonstrated that both AgNPs and CuNPs enhanced secondary metabolite production, including saponins and alkaloids. CuNPs consistently showed stronger stimulatory effects than AgNPs at all tested concentrations, with peak responses observed at 40–50 mg/L. The findings indicate that CuNPs are more effective elicitors of bioactive compound accumulation, while AgNPs also contribute positively, though to a lesser extent.

Overall, this study highlights the dual potential of green-synthesized nanoparticles: as safe, effective growth inducers and as potent elicitors for enhancing valuable phytochemicals in medicinal plants, providing a promising strategy for plant biotechnology and nanobiotechnolog applications.

Green–synthesized AgNPs and CuNPs effectively enhanced secondary metabolite accumulation, including phenolics, flavonoids, saponins, and alkaloids, in *Bacopa monnieri*, with CuNPs consistently showing stronger effects than AgNPs. Both nanoparticles induced a concentration–dependent rise in oxidative stress markers (H_2O_2, MDA) and stimulated antioxidant enzymes (CAT, APX, SOD) and PAL activity, indicating that ROS–mediated signaling drives the observed enhancement in secondary metabolism. Overall, CuNPs act as more potent elicitors of bioactive compounds and antioxidant defense in *B. monnieri*, demonstrating their potential in plant nanobiotechnology applications.

CuNPs strongly induced oxidative stress, enhancing PAL activity, phenolics, flavonoids, and antioxidant capacity in *Bacopa monnieri*, whereas AgNPs had minimal effect on PAL and ROS-mediated pathways but effectively increased bacoside accumulation. These results highlight the nanoparticle-specific responses: CuNPs act as potent elicitors of phenylpropanoid metabolism and antioxidant defense, while AgNPs selectively stimulate triterpenoid saponin (bacoside) biosynthesis without causing oxidative stress. CuNPs act as strong elicitors in *Bacopa monnieri*, inducing ROS generation, enhancing antioxidant enzymes (CAT, APX, SOD), and stimulating secondary metabolite accumulation. In contrast, AgNPs show minimal activation of antioxidant defenses, with limited ROS signaling and weaker effects on secondary metabolism, indicating nanoparticle-specific physiological responses.

References

[1] Pathak P, Verma S.K. Green Synthesis of Copper Nanoparticles (CuNPs) and their Significance with Respect to Antibacterial and Anti-Cancer Activity. *Int. J. Pharm. Sci. Rev. Res.* 2023;80(2):152-160.
[2] Zhang Y, Cui L, Lu Y, et al. Characterization of Silver Nanoparticles Synthesized by Leaves of Lonicera japonica Thunb. *Int. jou. nanomedicine.* 2022; 17: 1647–1657.
[3] Kishor A, Jadon G. Neuroprotective Evaluation of *Bacopa monnieri*-Loaded Chitosan Nanoparticles: A Green Chemistry Approach. *Int. J. Environ. Sci.* 2025;11(6):1245-1258.
[4] Murashige T, Skoog F. A Revised Medium for Rapid Growth and Bio Assays with Tobacco Tissue Cultures. *Physiol Plantarum*. 1962; 15: 473-497.
[5] Sreevidya N, Mehrotra S. Spectrophotometric method for estimation ofalkaloids precipitated by Dragendorff's reagent in plant materials. *J. AOACInt.* 2003;86(3):1124–1127.
[6] Bhardwaj P, Jain CK, Mathur A. Comparative qualitative andquantitative analysis of phytochemicals in five different herbal formulations of *Bacopa monnieri*. *Int. J. Pharmacogn. Phytochem. Res.* 2016;8(4):675–682.
[7] Ainsworth EA, Gillespie KM. Estimation of total phenolic content and other oxidation substrates in plant tissues using Folin–Ciocalteu reagent. *Nature Protocols*. 2007; 2: 875–877.
[8] Hassan SM, Al-Aqil AA, Attimarad M. Determination of crude saponinand total flavonoids content in guar meal. *Adv. Med. Plant Res.* 2013;1(1):24–28.

[9] Sykłowska-Baranek K, Pietrosiuk A, Naliwajski MR, et al. Effect of l phenylalanine on PAL activity and production of naphthoquinone pigments in suspension cultures of Arnebia euchroma (Royle) Johnst. *In Vitro Cell. Dev. Biol. Plant.* 2012; 48: 555–564.
[10] Chen GX, Asada K. Ascorbate peroxidase in tea leaves: occurrence of two isozymes and the differences in their enzymatic and molecular properties. *Plant Cell Physiol.* 1989;30(7):987–998.
[11] Bienert GP, Schjoerring JK, Jahn TP. Membrane transport of hydrogenperoxide', Biochim. *Biophys. Acta.* 2006; 1758: 994–1003.
[12] Dai Y, Wang W, Zhao J et al. Interaction of CuO nanoparticles withplant cells: internalization, oxidative stress, electron transport chaindisruption, and toxicogenomic responses. *Environ. Sci. Nano.* 2018; 5: 2269–2281.
[13] Qian H, Peng X, Han X, et al. Comparison of the toxicity of silver nanoparticles and silver ions on the growth of terrestrial plant model Arabidopsis thaliana. *J. Environ. Sci.* 2013; 25: 1947–1956.
[14] Zhao L, Hu Q, Huang Y, et al. 'Response at genetic, metabolic, and physiological levels of maize (Zea mays) exposed to a Cu(OH)2 nanopesticide'. *ACS Sustainable Chem. Eng.* 2017;5(9):8294–8301.
[15] Santala KR, Ryser P. Influence of heavy-metal contamination on plant response to water availability in white birch, Betula papyrifera. *Environ. Exp. Bot.* 2009; 66: 334–340.
[16] Khatun S, Ali MB, Hahn EJ, et al. Botany E. Copper toxicity in Withania somnifera: Growth and antioxidant enzymes responses of in vitro grown plants. *Environ. Exp. Bot.* 2008; 64: 279–285.
[17] Mittler R. Oxidative stress, antioxidants and stress tolerance. *Trends Plant Sci.* 2002; 7: 405–410.
[18] De La Torre-Roche R, Hawthorne J, Musante C, et al. Impact of Ag nanoparticle exposure on p,p'-DDE bioaccumulation by Cucurbita pepo (zucchini) and Glycine max (soybean). Environ Sci Technol. 2013;47(2):718-725. doi:10.1021/es3041829
[19] Lin TH. Huang YL, Huang SF. Lipid peroxidation in liver of rats administrated with methyl mercuric chloride. *Biol. Trace Elem. Res.* 1996; 54: 33–41.
[20] Thiruvengadam M, Gurunathan S, Chung IM. Physiological, metabolic, and transcriptional effects of biologically-synthesized silver nanoparticles in turnip (Brassica rapa ssp. rapa L.). *Protoplasma.* 2015; 252: 1031–1046.
[21] Khosropour E, et al. Silver nanoparticle-mediated enhancement of secondary metabolites in medicinal plants: *A review. Plant Cell Reports.* 2020; 39: 1441–1457.
[22] Khan MN, et al. Copper nanoparticles induce oxidative stress and physiological changes in plants. *Environ. Nanotechnol. Monit & Managem.* 2021; 15: 100431.
[23] Tripathi DK, Shweta, Singh S, et al. Nanoparticles and plant responses. *Plant Physiol. Biochem.* 2017; 110: 2–12.
[24] Rajput, V. D., et al. (2018). Nanotechnology and plant stress responses. Plant Physiology Reports, 23, 1–15.
[25] Faizan, M., et al. (2020). CuO nanoparticles-induced oxidative stress and biochemical responses in plants. Ecotoxicology and Environmental Safety, 190, 110106.
[26] Kralova K, Jampilek J. Responses of medicinal and aromatic plants to engineered nanoparticles. *Applied Sciences.* 2021;11(4):1813.
[27] Lala S. Enhancement of secondary metabolites in *Bacopa monnieri* (L.) Pennell plants treated with copper-based nanoparticles in vivo. *IET Nanobiotechnol*. 2019;14(1):78–85.